DALTON

Exchange couplings and hydrogen dynamics in ruthenium trihydride adducts with coinage-metal cations†

Blanca Manzano,[a] Felix Jalon,[a] Jochen Matthes,[b] Sylviane Sabo-Etienne,[b] Bruno Chaudret,*[,b] Stefan Ulrich[c] and Hans-Heinrich Limbach*[,c]

[a] *Departamento de Quimica Inorganica, Organica y Bioquimica, Universidad de Castilla-La Mancha, Campus Universitario, 13071 Ciudad Real, Spain*
[b] *Laboratoire de Chimie de Coordination CNRS, 205 Route de Narbonne, 31077 Toulouse-Cedex, France*
[c] *Freie Universität Berlin, Fachbereich Chemie, Institut für Organische Chemie, Takustrasse 3, D-14195 Berlin, Germany*

The reactions of $AgBF_4$ and $[Au(tht)_2]PF_6$ with $[Ru(\eta\text{-}C_5Me_5)H_3\{P(C_6H_{11})_3\}]$ **1** (tht = tetrahydrothiophene) led to the adducts $[\{Ru(\eta\text{-}C_5Me_5)H_3[P(C_6H_{11})_3]\}_2M]X$ (M = Ag, X = BF_4 **3**; M = Au, X = PF_6 **4**) similar to the previously reported $[\{Ru(\eta\text{-}C_5Me_5)H_3[P(C_6H_{11})_3]\}_2Cu]PF_6$ **2**. Variable-temperature ^{1}H NMR experiments were performed on **2**–**4** dissolved in organic liquids down to 130 K which complement previous experiments on **1**. Like **1** and **2**, **3** and **4** display at low temperatures exchange couplings between proton pairs in the trihydride sites which increase with temperature and which depend on the molecular structure. At higher temperatures a classical exchange between the hydride protons occurred the rate constants for which determined by lineshape analysis. As the coinage metal lowers the symmetry of the trihydride spin systems from the AB_2 type in **1** to the ABC type in **2**–**4**, the ^{1}H NMR spectra also give information about the rate constants of an intramolecular metal transfer leading to an effective AB_2 symmetry of the trihydride spins. The results indicate (*i*) the absence of kinetic hydrogen/deuterium isotope effects on the classical hydrogen-exchange processes within the margin of error in the temperature interval covered, (*ii*) only small effects of the presence of Lewis-acidic cation on the classical exchange dynamics, but (*iii*) important effects of these cations on the quantum-mechanical exchange couplings. In particular, these couplings increase with increasing electronegativity of the coinage metal by favouring dihydrogen configurations.

The presence of very large H–H couplings in the NMR spectra of certain transition-metal hydrides L_nMH_3 has stimulated an intense research effort from experimental and theoretical chemists.[1–11] These couplings arise from quantum-mechanical dihydrogen exchange corresponding to a coherent tunnel process.[6] They were first reported for ruthenium trihydrides at low temperatures[1] and later for a variety of other metal trihydride systems which all exhibit a similar molecular plane containing the metal and the hydride ligands.[2–4] Exchange couplings between only two hydride sites have been observed in the case of mono-deuteriated and -tritiated trihydrides L_nMH_2D and L_nMH_2T, various Lewis-acid adducts with coinage metals $(L_nMH_3)_2X^+$, and recently in the case of cationic transition-metal complexes $(\eta\text{-}C_5H_5)_2TaH_2L^{+5}$ containing two hydrides in a mutual *cis* position or a stretched co-ordinated dihydrogen ligand. Evidence for a similar phenomenon was also gained in cationic niobium derivatives.[12]

Exchange couplings strongly increase with increasing temperature until they can no longer be observed because they become either much larger than the associated chemical shift differences and/or because of the onset of a classical dihydrogen exchange process which can also be viewed as a hindered rotation. This process is incoherent and can be described by rate constants. Therefore, it leads to the usual line broadening and coalescence. The quantum-mechanical nature of the exchange-coupling phenomenon has been demonstrated[6,7] but a more detailed picture of the physical processes accounting for these couplings and for the transition from the quantum to the classical dihydrogen exchange regime remains open to discussion.[6–8,10] For example, little is known about the question whether in these systems the classical exchange exhibits hydrogen/deuterium isotope effects, as do many other double proton-transfer reactions.[13] Preliminary observations in the case of $[Ta(\eta\text{-}C_5H_5)_2H_2\{P(OMe)_3\}]^+$ indicated surprisingly small effects,[5b] whereas the absence of a kinetic isotope effect in the fluxionality of $[ReH_2(CO)(NO)(PR_3)_2]$, a compound not displaying exchange couplings, has been previously demonstrated.[14]

Some of us have previously suggested a link between the quantum and classical exchange and the presence of a low-lying dihydrogen state in the complexes displaying exchange couplings.[8] For example, *ab initio* calculations gave evidence for the presence of a hydridodihydrogen state in niobium trihydrides displaying such couplings, whereas this state is located at much higher energy in the case of the isoelectronic and isostructural tantalum trihydrides which do not exhibit these couplings.[9] Further evidence is the role of electron-withdrawing ligands which favour the dihydrogen state and increase the exchange couplings.

The role of the influence of electron-withdrawing coinage metals acting as Lewis acids in complexes $(L_nMH_3)_2X^+$ is, therefore, of special interest. In the case of M = Nb it was observed that replacing X = Cu by Au led to a remarkable increase of the quantum exchange couplings.[2b,c] Therefore, we decided to study systematically the effects of various coinage metals on the quantum exchange and the classical dihydrogen exchange, as compared to the parent compound studied previously.[8b] In particular, we chose the system $[\{Ru(\eta\text{-}C_5Me_5)H_3[P(C_6H_{11})_3]\}_2X]^+$ (X = Cu^+, Ag^+ or Au^+). The synthesis and NMR spectroscopy of the parent compound $[Ru(\eta\text{-}C_5Me_5)H_3\{P(C_6H_{11})_3\}]$ and of its copper adduct have been reported previously.[1c] Here we describe the synthesis and characterization of new adducts with

† Dedicated to Professor Sir Geoffrey Wilkinson for his outstanding contribution to inorganic chemistry and as an expression of personal gratitude to him.

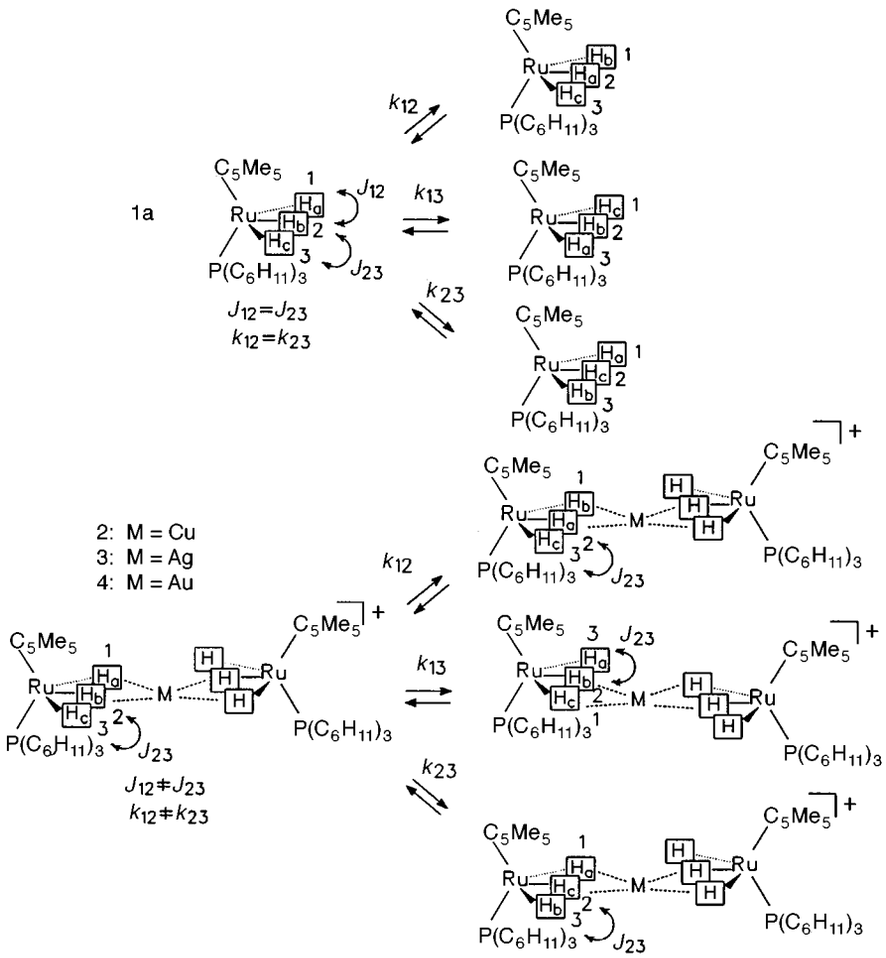

Fig. 1 Exchange processes in compounds **1** to **4**

Ag^+ and Au^+ together with dynamic NMR experiments performed on the adducts and on the parent compound as a reference. The results indicate the presence of a relationship between the electronegativity of the coinage metal and the magnitude of the exchange couplings. Moreover, the rate constants of the classical exchange process (see Fig. 1) were determined by lineshape analysis. Experiments on the partially and fully deuteriated isotopomers of **1** were carried out in order to determine the kinetic hydrogen/deuterium isotope effects on the classical exchange process in this compound. As these effects were small we did not extend these measurements to the adducts.

We report first the synthesis of the novel adducts and their structural characterization. Then the NMR experiments are described and the results discussed.

Results

Synthesis of the complexes

The synthesis of $[\{Ru(\eta\text{-}C_5Me_5)H_3[P(C_6H_{11})_3]\}_2Cu]PF_6$ **2** from **1** and $[Cu(MeCN)_4]PF_6$ has been previously reported.[1c] Similarly, the reaction of **1** with $AgBF_4$ in tetrahydrofuran (thf) produces the adduct $[\{Ru(\eta\text{-}C_5Me_5)H_3[P(C_6H_{11})_3]\}_2Ag]BF_4$ **3** which can be isolated as white crystals in 75% yield after recrystallization from thf–diethyl ether. The reaction of **1** with $[Au(tht)_2]PF_6$ (tht = tetrahydrothiophene) leads to $[\{Ru(\eta\text{-}C_5Me_5)H_3[P(C_6H_{11})_3]\}_2Au]PF_6$ **4** which can be isolated in 54% yield as white crystals after recrystallization from thf–diethyl ether.

Compounds **2**–**4** all show infrared bands attributed to terminal hydrides respectively at 2005m (sh) (**2**), 2030m (sh) (**3**) and 2019m (sh) cm^{-1} (**4**) together with bands attributed to bridging hydrides at 1790m (br) (**2**), 1789m (br) (**3**) and 1736m (br) cm^{-1} (**4**). The new complexes **3** and **4** each show a single peak in their ^{31}P NMR spectra respectively at δ 80.2 and 77.9 in $(CD_3)_2CO$, close to the value found for **1** (δ 83.9 in C_6D_6). The hydride signals consist in each case at room temperature of a doublet due to the coupling of the three equivalent hydrides with phosphorus, respectively at δ −10.94 [*J*(H–P) 22.5 Hz; **1**, C_6D_6], −10.38 [*J*(H–P) 14.5 Hz; **2**, $(CD_3)_2CO$], −9.75 [*J*(H–P) 15.7 Hz; **3**, $(CD_3)_2CO$] and −7.32 [*J*(H–P) 13.6 Hz; **4**, $(CD_3)_2CO$]. In the case of **3** the hydride signal is split by couplings to the ^{107}Ag and ^{109}Ag isotopes. However, the different couplings are not resolved and only a mean value is observed [*J*(H–Ag) 48.6 Hz]. These data clearly indicate that the three adducts display a similar structure which, as far as the ruthenium moiety is concerned, is not very different from that of **1**. The modification of the chemical shift of the hydride signal may be due to a shielding effect by the electrons of gold and silver whereas the reduction of the P–H couplings may result from a lengthening of the Ru–H distances and modification of the P–Ru–H angles upon co-ordination to the coinage-metal cations. However, these four compounds were shown to exhibit different NMR behaviours at low temperature. The variation of their exchange couplings as well as their classical fluxionality were then studied.

Dynamic NMR experiments

In this section we report the results of the lineshape analyses of the variable-temperature NMR spectra of compounds **2**–**4** (Fig. 1). The lineshapes give information about the exchange couplings and the rate constants of the various processes shown in Fig. 1. Each compound contains different nuclear sites *i*, *j* = 1–5 characterized by the chemical shifts δ_i, containing the nuclei H_a, H_b, H_c, ^{31}P and in one case ^{107}Ag and ^{109}Ag. The coupling constants between two nuclei in the sites *i* and *j* are

Table 1 Parameters of the 500 MHz ^{1}H NMR lineshape analyses of [{Ru(η-C_5Me_5)H_3[P(C_6H_{11})$_3$]}$_2$Cu]PF_6 **2** dissolved in [$^2H_8$]tetrahydrofuran

T/K	ν_1/Hz	ν_2/Hz	ν_3/Hz	W_0/Hz	J_{12}/Hz	J_{23}/Hz	k_{12}/s^{-1}	k_{13}/s^{-1}	k_{23}/s^{-1}
187	−5 228	−6 010	−4 616	30	−10	45			
197	−5 225	−6 012	−4 610	20	−10	60		50	
207	−5 220	−6 010	−4 615	18	−10	85		200	
217	−5 170	−6 002	−4 650	15	−5	112	25	450	25
227	−5 125	−5 998	−4 690	15	30	120	30	500	50
237	−5 100	−5 990	−4 690	10	50	150	150	800	200
247	−5 120	−5 990	−4 660	10	50	174*	500	2 500	600
257	−5 120	−5 990	−4 660	10	50	205*	1 200	15 000	1 800
267	−5 120	−5 990	−4 660	10	50	238*	4 000	30 000	3 000
287	−5 120	−5 990	−4 660	10	50	312*	30 000	90 000	10 000

* Extrapolated from low temperatures.

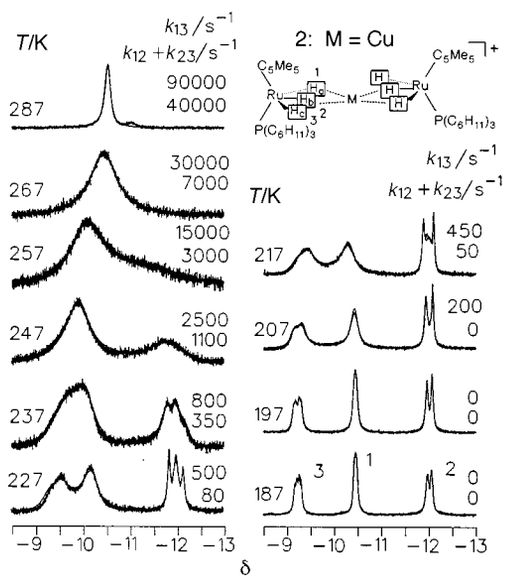

Fig. 2 Superimposed temperature-dependent experimental and calculated 500 MHz ^{1}H NMR hydride signals of [{Ru(η-C_5Me_5)H_3[P(C_6H_{11})$_3$]}$_2$Cu]PF_6 **2** dissolved in [$^2H_8$]tetrahydrofuran

labelled as J_{ij}. The NMR spectra of **2**–**4** depend on the rate constants k_{ij} characterizing the process where in the initial state one nucleus experiences the chemical shift δ_i (frequency ν_i) and the other δ_j (ν_j), whereas in the final state the chemical shifts are reversed. There are three hydride sites i, j = 1–3 in compounds **2** to **4**. The hydrogen nuclei in these sites can be labelled by their nuclear spin, and, therefore, subscripts a–c are included in Fig. 1. The ^{31}P nucleus is located in site 4 and the coinage metal in site 5. All parameters of the lineshape analyses are assembled in Tables 1 to 5.

[Ru(η-C_5Me_5)H_3{P(C_6H_{11})$_3$}] 1. The NMR spectroscopy of compound **1** and its partially deuteriated isotopomers has been described recently.[8b] Expressions (1) and (2) were derived. These

$$\pi J_{12} = 10^{4.3} \exp(-7.1 \text{ kJ mol}^{-1}/RT) \text{ Hz};$$
$$220 < T < 280 \text{ K}, J_{12}(240 \text{ K}) = 181 \text{ Hz} \quad (1)$$

$$k_{12} = 10^{14.6} \exp(-55.5 \text{ kJmol}^{-1}/RT);$$
$$220 < T < 280 \text{ K}, k_{12}(240 \text{ K}) = 330 \text{ s}^{-1} \quad (2)$$

data are valuable for comparison with those obtained for the coinage adducts described in the following.

[{Ru(η-C_5Me_5)H_3[P(C_6H_{11})$_3$]}$_2$Cu]PF_6 2. In Fig. 2 are shown the superimposed calculated and experimental ^{1}H NMR signals of compound **2** dissolved in [$^2H_8$]tetrahydrofuran. At low temperature typical ABCX signal patterns are observed for the hydrides in the three sites. A coupling to ^{31}P (site 4) is resolved only for site 3, with J_{34}(H–P) = J_{34} = 25 Hz. The signals arising from sites 2 and 3 exhibit large exchange couplings J_{23} which increase with temperature. Above 217 K the signals of sites 1 and 3 broaden and coalesce because of the above-mentioned site interconversion (see also Fig. 1); at the same time a doublet–triplet transition is observed for the signal of site 2. This observation indicates that Cu is bound relatively strongly to the hydride in site 2 and more weakly to the proton in site 1. We note that the spectra could not be simulated in a satisfactory way without assuming a substantial exchange coupling J_{13}. Above 237 K the signal of the hydride in site 2 also broadens because of exchange with sites 1 and/or 3, and eventually a single line is observed at room temperature because of fast exchange between all three hydride sites. The temperature dependency of the parameters obtained by lineshape analysis can be expressed as in equations (3)–(5).

$$\pi J_{23} = 10^{4.56} \exp(-8.6 \text{ kJ mol}^{-1}/RT) \text{ Hz};$$
$$187 < T < 237 \text{ K}, J_{12}(240 \text{ K}) = 170 \text{ Hz} \quad (3)$$

$$k_{13} = 10^{12.1} \exp(-39.8 \text{ kJ mol}^{-1}/RT) \text{ s}^{-1};$$
$$207 < T < 287 \text{ K}, k_{13}(240 \text{ K}) = 2700 \text{ s}^{-1} \quad (4)$$

$$k_{12} + k_{23} = 10^{13.9} \exp(-51.1 \text{ kJ mol}^{-1}/RT) \text{ s}^{-1};$$
$$217 < T < 287 \text{ K}, (k_{12} + k_{23})(240 \text{ K}) = 590 \text{ s}^{-1} \quad (5)$$

[{Ru(η-C_5Me_5)H_3[P(C_6H_{11})$_3$]}$_2$Ag]BF_4·2Et_2O 3. In Fig. 3 are shown the superimposed calculated and experimental ^{1}H NMR signals of compound **3** dissolved in $CDClF_2$–CDF_3. At low temperature two high-order multiplets are observed. The signal at δ −11 is assigned to site 2 which is coupled to the two silver isotopes ^{107}Ag and ^{109}Ag, present in the atom fraction 0.5182/0.4818. The coupling constants are J_{25}(H–^{107}Ag) = 70 and J_{25}(H–^{109}Ag) = 80.7 Hz. The proton in site 2 exhibits a large exchange coupling with the proton in site 3, characterized by J_{23}, but the coupling constant J_{12} cannot be resolved. The high-order multiplet at δ −9.3 consists of two superimposed signals arising from the protons in sites 1 and 3. The proton in site 1 is only coupled to the phosphorus nuclei by J_{14}(H–P) = 20 Hz and to the silver isotopes by J_{15}(H–^{107}Ag) = 74 and J_{15}(H–^{109}Ag) = 85 Hz. The proton in site 3 contributes an AB-type doublet to the spectrum characterized by J_{23}, where each component is further split by coupling with the phosphorus nucleus by J_{34}(H–P) = 14 Hz. Again a strong increase of J_{23} with increasing temperature is observed. Above 154 K the signals of the protons in sites 1 and 3 broaden and coalesce. Despite the broadening of the proton in site 2 it is possible to obtain the exchange coupling J_{23} by lineshape analysis in a wide temperature range up to 226 K since k_{23}^{HH} does not increase strongly with temperature. The temperature dependency of the parameters obtained is given by expressions (6)–(8).

$$\pi J_{23} = 10^{5.5} \exp(-7.3 \text{ kJ mol}^{-1}/RT) \text{ Hz};$$
$$134 < T < 226 \text{ K}, J_{12}(240 \text{ K}) = 2590 \text{ Hz} \quad (6)$$

Table 2 Parameters of the 500 MHz ^{1}H NMR lineshape analyses of [{Ru(η-C_5Me_5)H_3[P(C_6H_{11})$_3$]}$_2$Ag]BF_4·2Et_2O **3** dissolved in $CDClF_2$–CDF_3 (2:1)

T/K	ν_1/Hz	ν_2/Hz	ν_3/Hz	W_0/Hz	J_{23}/Hz	k_{12}/s^{-1}	k_{23}/s^{-1}
134	−4 560	−5 507	−4 695	30	150		≈80
144	−4 540	−5 500	−4 690	30	217		≈80
154	−5 430	−5 495	−4 690	30	280		≈80
165	−4 520	−5 485	−4 700	30	370	50	100
175	−4 520	−5 475	−4 700	30	480	300	200
184	−4 510	−5 465	−4 690	10	700	800	400
194	−4 515	−5 455	−4 695	10	1 000	3 000	500
206	−4 510	−5 445	−4 690	10	1 300	12 000	600
216	−4 515	−5 455	−4 695	10	1 800	20 000	700
226	−4 510	−5 440	−4 690	10	2 000	25 000	1 500

Heteronuclear scalar coupling constants: J_{15}(^{1}H–^{107}Ag) = 74; J_{15}(^{1}H–^{109}Ag) = 85.7, J_{25}(^{1}H–^{107}Ag) = 70, J_{25}(^{1}H–^{109}Ag) = 80.7, J_{14}(H–P) = 14, J_{24}(H–P) = 20 Hz.

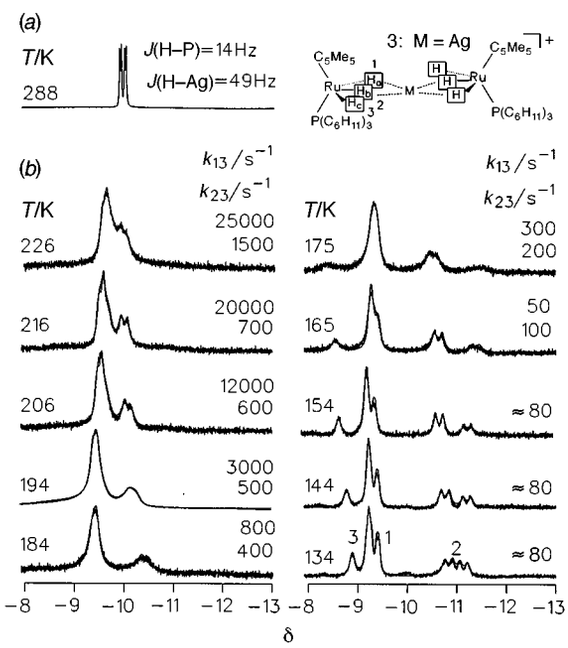

Fig. 3 Superimposed temperature-dependent experimental and calculated 500 MHz ^{1}H NMR hydride signals of [{Ru(η-C_5Me_5)H_3[P(C_6H_{11})$_3$]}$_2$Ag]BF_4·2Et_2O **3** dissolved in $CDCl_2$ (*a*) and in $CDClF_2$–CDF_3 (2:1) (*b*)

$$k_{13} = 10^{12.2} \exp(-32.6 \text{ kJ mol}^{-1}/RT) \text{ s}^{-1};$$
$$165 < T < 226 \text{ K}, k_{13}(240 \text{ K}) = 126\,000 \text{ s}^{-1} \quad (7)$$

$$k_{23} = 10^{5.9} \exp(-12 \text{ kJ mol}^{-1}/RT) \text{ s}^{-1};$$
$$165 < T < 226 \text{ K}, k_{23}(240 \text{ K}) = 244 \text{ s}^{-1} \quad (8)$$

[{Ru(η-C_5Me_5)H_3[P(C_6H_{11})$_3$]}$_2$Au]PF_6 4. In Fig. 4 are shown the superimposed calculated and experimental ^{1}H NMR signals of compound **4** dissolved in $CDClF_2$–CDF_3. At low temperature we observe a broad singlet at δ −5.8 for the proton in site 1 and another broad line at δ −8 for the protons in sites 2 and 3 which splits below 175 K. The splitting increases as the temperature decreases and is assigned to the two inner lines of an AB spin system, where the exchange coupling is so large that the outer lines *i.e.* J_{23} can no longer be observed. In order to obtain the latter by lineshape analysis, the frequency difference $\Delta\nu = \nu_2 - \nu_3$ must be known. In order to evaluate Δν we deuteriated **4** in the hydride sites and were able to observe three singlets for the protons in sites 1 to 3 of [$^2H_2$]**4** at δ_1 −6.0, δ_2 −9.1 and δ_3 −7.3 as shown in Fig. 4 (bottom, right-hand side; the presence of the residual, non-deuteriated complex **4** is observed at δ −8.1). Neglecting possible H/D isotope effects on the hydride chemical shifts we were then able to calculate the values

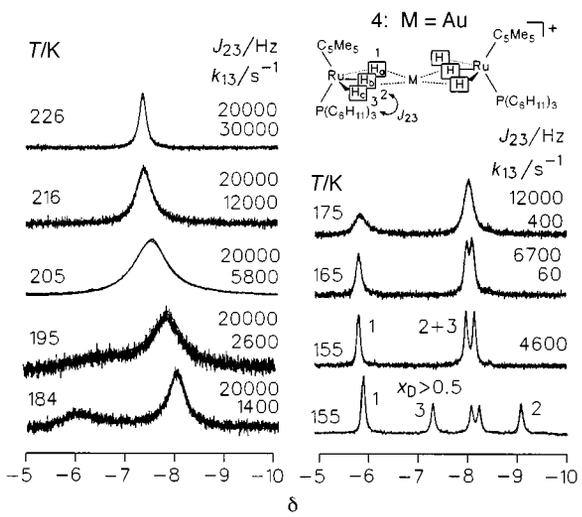

Fig. 4 Superimposed temperature-dependent experimental and calculated 500 MHz ^{1}H NMR hydride signals of [{Ru(η-C_5Me_5)H_3[P(C_6H_{11})$_3$]}$_2$Au]PF_6 **4** dissolved in $CDClF_2$–CDF_3 (2:1)

of the exchange couplings J_{23} in a limited temperature range, equation (9). Above 175 K all signals broaden and coalesce

$$\pi J_{23} = 10^{8.2} \exp(-12.1 \text{ kJ mol}^{-1}/RT) \text{ Hz};$$
$$155 < T < 184 \text{ K}, J_{12}(240 \text{ K}) = 117\,300 \text{ Hz} \quad (9)$$

because of the interconversion between site 1 and 3, and the rate constants k_{13} could be determined, equation (10).

$$k_{13} = 10^{11.3} \exp(-29.5 \text{ kJ mol}^{-1}/RT) \text{ s}^{-1};$$
$$165 < T < 226 \text{ K}, k_{13}(240 \text{ K}) = 75\,000 \text{ s}^{-1} \quad (10)$$

Discussion

We have shown that ruthenium trihydride complexes form adducts with metal ions such as Cu^+, Ag^+ and Au^+. The structure of these adducts is asymmetric, *i.e.* the coinage metal is preferentially bonded to the outer hydride sites, and partially to the central hydride site. These bonds are fluxional and a rapid bond-breaking bond-formation process between the two outer hydrides and the coinage metal is observed, leading to an exchange of the two outer hydride sites. Moreover, the bonding to the coinage metal does not hinder quantum and classical exchange between the hydride sites. The structures of the adducts were characterized by different spectroscopic techniques. Extended NMR studies were carried out on **1** to **4** as well as on the deuteriated analogues of **1** from which some novel insights into the mechanisms of the various hydrogen-exchange processes are obtained. In this section we first discuss

Table 3 Parameters of the 500 MHz ^{1}H NMR lineshape analyses of [{Ru(η-C_5Me_5)H_3[P(C_6H_{11})$_3$]}$_2$Au]PF_6 **4** dissolved in $CDClF_2$–CDF_3 (2:1)

T/K	ν_1/Hz	ν_2*/Hz	ν_3*/Hz	W_0/Hz	J_{23}/Hz	k_{13}/s^{-1}
155	−2 932	−4 481	−3 605	40	4 600	
165	−2 935	−4 480	−3 605	35	6 700	60
175	−2 945	−4 470	−3 605	35	12 000	400
184	−2 932	−4 460	−3 605	20	20 000	1 400
195	−2 932	−4 450	−3 605	5	20 000	2 600
205	−2 932	−4 440	−3 605	5	20 000	5 800
216	−2 932	−4 430	−3 605	5	20 000	12 000
226	−2 932	−4 420	−3 605	5	20 000	30 000

* Extrapolated from values for [$^2H_2$]**4** (see Table 5) as described in the text.

Table 4 Parameters of the 500 MHz ^{1}H NMR lineshape analyses of [{Ru(η-C_5Me_5)H_2D[P(C_6H_{11})$_3$]}$_2$Au]PF_6 [$^2H_2$]**4** dissolved in $CDClF_2$–CDF_3 (2:1)

T/K	ν_1/Hz	ν_2/Hz	ν_3/Hz	W_0/Hz	k_{12}/s^{-1}	k_{13}/s^{-1}	k_{23}/s^{-1}
155	−2983	−4540*	−3671*	40	0	0	0

* Extrapolated from values for [$^2H_2$]**4** (see Table 5) as described in the text.

Table 5 Parameters of the 500 MHz ^{1}H NMR lineshape analyses of [{Ru(η-C_5Me_5)H_2D[P(C_6H_{11})$_3$]}$_2$Au]PF_6 [$^2H_2$]**4** dissolved in $CDClF_2$–CDF_3 (2:1)

T/K	ν_1/Hz	ν_2/Hz	ν_3/Hz	W_0/Hz	J_{12}/Hz	k_{12}/s^{-1}	k_{13}/s^{-1}	k_{23}/s^{-1}
155	−2983	−4540	−3671	40	4800	0	0	0

the structural variations induced by the bonding to the coinage metal cations, the dynamics of the intramolecular metal transfer in the adducts, and then the metal influence on the classical and quantum hydrogen-exchange dynamics.

Effects of coinage-metal cations on the structure of ruthenium trihydrides and on the dynamics of the intramolecular coinage-metal cation transfer in the adducts

The asymmetry of the structure is confirmed at low temperatures by NMR spectroscopy as the three hydrides form ABC spin systems exhibiting different chemical shifts. This indicates metal binding preferentially to the external hydride sites and to the central hydride. In principle one would expect the presence of two isomers with a *cis*- and a *trans*-ligand structure with respect to the coinage-metal cation. However, only one form was observed indicating either the presence of the *cis* or of the *trans* isomer.

The binding of the metal cation M^+ to the external and central hydride is not static but fluxional as revealed by the NMR spectra of compounds **2** to **4**. Without dissociation, the bond of M^+ to the external hydride can be broken and reformed again with the other external hydride. As only one isomer was observed the process corresponds to a stepwise or concerted rearrangement of both ruthenium atoms around the coinage-metal cation, or of a coinage-metal transfer between the hydride sites. The resulting Arrhenius diagram is depicted in Fig. 5. First we note that preexponential factors typical for intramolecular reactions of the order of 10^{11}–10^{13} s^{-1} are observed. The energy of activation is substantially larger for the complex with Cu^+ as compared to the complexes with Ag^+ and Au^+ which have similar binding energies indicating a more Lewis-acidic character of Cu^+.

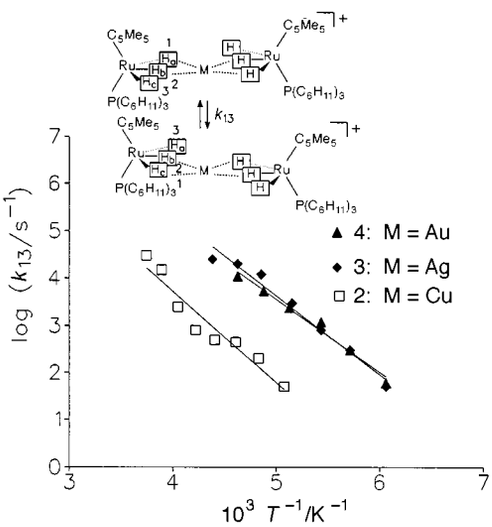

Fig. 5 Arrhenius diagram of the interconversion between sites 1 and 3 in compounds **2**–**4** dissolved in [$^2H_8$]tetrahydrofuran **2** and $CDClF_2$–CDF_3 (**3**, **4**)

Quantum or coherent dihydrogen exchange in ruthenium trihydrides and the adducts with coinage-metal cations

The logarithms of the quantum exchange couplings J_{23} of compounds **1** to **4** are plotted in Fig. 6 as a function of the inverse temperature. We obtain fairly linear dependencies within the relatively small temperature ranges where the couplings could be observed. It is interesting that the influence of the addition of Cu^+ which forms the strongest bond with the hydrides does not lead to a substantial change of the couplings. By contrast, the addition of Ag^+ leads to a strong enhancement of the couplings, and the effect is even more pronounced in the case of Au^+. This finding can be interpreted as follows. In the series Cu^+, Ag^+, Au^+ the negative charge of the hydrides is gradually reduced which favours dihydrogen configurations. The formation of these configurations has been proposed to be responsible for these couplings.[8a] Within the framework of this proposition the increase of the exchange couplings with the electronegativity of the coinage-metal atom is not surprising.

Classical or incoherent dihydrogen exchange in ruthenium trihydrides and the adducts with coinage-metal cations

The effect of the coinage-metal cations on the classical exchange rates k_{23} is depicted in the Arrhenius diagram of Fig. 7. We are not surprised to find that the rate constants of compounds **1** and **2** coincide more or less, and that there is a strong enhancement of the classical exchange rates for the silver adduct **3**. This finding correlates well with the result of Fig. 6

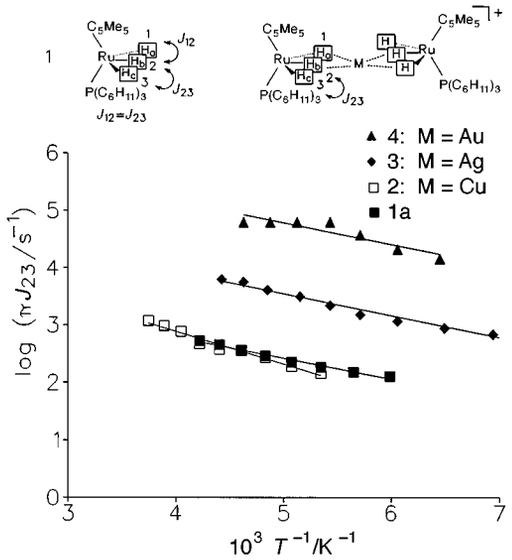

Fig. 6 Logarithms of the exchange couplings J_{23} of compounds **1**–**4** dissolved in [$^2H_8$]tetrahydrofuran (**1**, **2**) and $CDClF_2$–CDF_3 (**3**, **4**) as a function of the inverse temperature

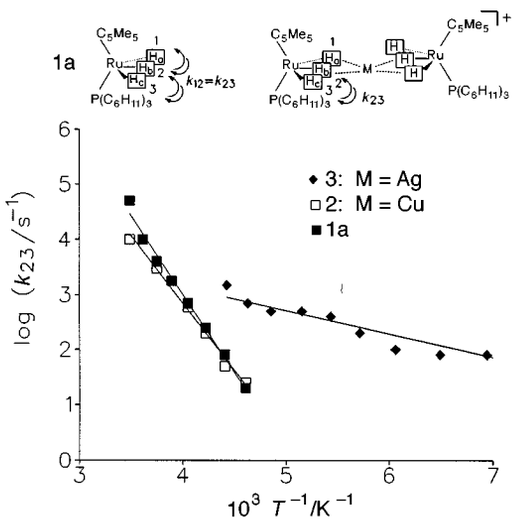

Fig. 7 Arrhenius diagram of the classical dihydrogen exchange between sites 2 and 4 in compounds **1**–**3** dissolved in [$^2H_8$]tetrahydrofuran (**1**, **2**) and $CDClF_2$–CDF_3 (**3**)

that the exchange couplings in **1** and **2** are similar, but strongly enhanced in **3**. The increase of the rate constants of **3** as compared to **1** arises from a substantial drop in the energy of activation. On the other hand, we also observe an anomalous decrease of the preexponential factor on the classical dihydrogen exchange (k_{23}) from about 10^{12} to 10^{14} s^{-1} for **1** and **2** to 10^6 s^{-1} for **3** [see equation (8)]. Without this decrease the increase of the rate constant would be extremely large. We were worried about the possibility of systematic errors in the lineshape analyses of Fig. 3 which could to some extent arise from transverse relaxation at low temperatures. Therefore, as a precaution, only rate constants above 165 K were included in the calculation of the Arrhenius parameters of equation (8), assuming absence of T_2 effects above this temperature which is supported by the finding that the rate constants k_{13} of the metal hopping process (Fig. 5) obtained from the same spectra do not show an anomalous small preexponential factor. At present, we can only speculate about the origin of the anomalous activation parameters of the classical dihydrogen exchange (k_{23}) in **3**. A clue to the understanding of this effect in the future may perhaps be the observation that the energies of activation describing the temperature dependency of log k_{23} and of log πJ_{23} *vs.* $1/T$ are similar in the case of **3**, but different for **1** and **2**. In the last cases the incoherent or classical exchange is determined by states close to the top of the barrier of the dihydrogen exchange or rotation, whereas the states which determine the exchange couplings are located at much lower energies. On the other hand, the similar energies of activation of the coherent and the incoherent exchange in **3** could then indicate that in this case both quantities are influenced in the temperature region covered by the same configuration or manifold of states, for example a low-lying dihydrogen configuration. If this explanation were true, one should expect a substantial kinetic HH/HD isotope effect on the low-temperature rate constants k_{23} of **3**. Such experiments are currently in progress.

Conclusion

We report in this study new adducts of ruthenium trihydrides with coinage metals. As previously observed in the case of copper and in the case of adducts with niobium trihydrides, the presence of Lewis-acidic cations does not impede the presence of exchange couplings. The magnitude of these couplings is related to the electronegativity of the coinage metal and a very strong increase is observed for the gold adduct (*ca.* 120 kHz at 240 K as compared to 181 Hz at 240 K in the case of **1**). A correlation could be observed between quantum-mechanical and classical exchanges. This correlation is a further confirmation that both processes are determined by the same rotation barrier.

Experimental

General procedures

All reactions and manipulations were carried out under Ar with use of standard inert-atmosphere and Schlenk techniques. Solvents were dried and distilled by standard procedures. The compounds [$Ru(\eta\text{-}C_5Me_5)H_3\{P(C_6H_{11})_3\}$][15] and [$Cu(MeCN)_4$]-$PF_6$[16] were synthesized by published procedures; [$Au(tht)_2$]PF_6 was synthesized from [AuCl(tht)], $AgPF_6$ and tht.[17] Silver tetrafluoroborate was obtained from Aldrich chemicals.

Preparation of NMR samples and instrumentation

For the low-temperature NMR experiments a liquified mixture of CDF_2Cl–CDF_3 (2:1) was used, prepared as described previously.[18] This solvent is fluid down to 90 K. The sealed NMR samples were prepared on a vacuum line using well described techniques.

The NMR spectra were recorded on Bruker spectrometers AM-250 (250 MHz) and AMX 500 (500 MHz). The chemical shifts δ are reported in the case of ^1H and ^2H with respect to $SiMe_4$ and in the case of ^{31}P with respect to an external 85% aqueous solution of H_3PO_4. The spectra were transferred to a personal computer where the lineshape analyses were performed using laboratory programs described previously, based on the quantum-mechanical density-matrix formalism of Binsch.[13,19] Infrared spectra were recorded as KBr discs in the range 4000–200 cm^{-1} on a PE683 spectrophotometer. Elemental analyses for C and H were performed on a PE 240B microanalyser.

Metal complex syntheses

[{Ru(η-C_5Me_5)H_3[P(C_6H_{11})$_3$]}$_2$Cu]PF_6 2. To a solution of compound **1** (0.400 g, 0.78 mmol) in thf (30 cm^3) was added [$Cu(MeCN)_4$]PF_6 (0.150 g, 0.40 mmol). The solution was stirred for 20 min at room temperature and then concentrated to *ca.* 5 cm^3. Diethyl ether was added until precipitation started. After cooling overnight **2** (0.192 g, 77%) was isolated by filtration as white crystals. ^1H NMR (295 K): δ −10.38 [d, 6 H, J (H–P) = 14.5 Hz, hydride; T_1 140 ms at 173 K, 75 ms at 203 K, 1.2–2.2 [m, 66 H, P(C_6H_{11})$_3$] and 2.23 (s, 30 H, C_5Me_5). IR

(cm^{-1}): 2005m (sh), 1790m (br) and 1710m (br), ν(Ru-H) [Found (Calc. for $C_{56}H_{102}CuF_6P_3Ru_2$): C, 53.95 (53.9); H, 8.9 (8.25)%].

[{Ru(η-C_5Me_5)H_3[P(C_6H_{11})$_3$]}$_2$Ag]BF_4·2Et_2O 3. To a solution of compound **1** (0.140 g, 0.27 mmol) in thf (10 cm^3) was added $AgBF_4$ (0.026 g, 0.14 mmol). The solution darkened very slightly and was stirred for 20 min at room temperature, filtered and concentrated to *ca.* 3 cm^3. Diethyl ether was added until precipitation started. After cooling overnight, **3** (0.141 g, 75%) was isolated by filtration as white crystals. ^{1}H NMR (295 K): δ −9.75 [dd, 6 H, *J*(H−P) = 15.7, *J*(H−Ag) = 48.6 Hz, hydride], 1.4–2.0 [m, 66 H, P(C_6H_{11})$_3$] and 2.25 (s, 30 H, C_5Me_5). The typical signals of diethyl ether have been observed. ^{31}P-{^{1}H} NMR: δ 80.22 (s). IR (cm^{-1}): 2030m (sh) and 1789m (br), ν(Ru−H) [Found (Calc. for $C_{64}H_{122}AgBF_4O_2P_2Ru_2$): C, 55.2 (55.1); H, 9.1 (8.75)%].

[{Ru(η-C_5Me_5)H_3[P(C_6H_{11})$_3$]}$_2$Au]PF_6 4. To a solution of compound **1** (0.170 g, 0.33 mmol) in thf (10 cm^3) cooled at −95 °C was added [Au(tht)$_2$]PF_6 (0.085 g, 0.17 mmol). The solution darkened slightly and was stirred for 15 min. The cooling bath was removed and the solution was filtered and partially evaporated to *ca.* 3 cm^3. Diethyl ether was added until precipitation started. After cooling overnight, **4** (0.120 g, 54%) was isolated as white crystals. ^{1}H NMR (295 K): δ −7.32 [d, 6 H, *J*(H−P) = 13.6 Hz, hydride], 1.2–2.2 [m, 66 H, P(C_6H_{11})$_3$] and 2.21 (s, 30 H, C_5Me_5). ^{31}P-{^{1}H} NMR: δ 77.93 (s). IR (cm^{-1}): 2019m (sh) and 1736m (br), ν(Ru−H) [Found (Calc. for $C_{56}H_{102}AuF_6P_3Ru_2$: C, 48.3 (48.7); H, 7.1 (7.5)%].

Acknowledgements

This work has been supported by Centre National de la Recherche Scientifique, by the European Union within the framework of the Human Capital & Mobility Network on 'Localization and Transfer of Hydrogen', the Deutsche Forschungsgemeinschaft, Bonn-Bad Godesberg, the PROCOPE Program of the Deutsche Akademische Austauschdienst, Bonn-Bad Godesberg, and by the Fonds der Chemischen Industrie, Frankfurt.

References

1 (*a*) T. Arliguie, B. Chaudret, J. Devillers and R. Poilblanc, *C. R. Hebd. Seances Acad. Sci., Ser. 2*, 1987, **305**, 1523; (*b*) T. Arliguie, C. Border, B. Chaudret, J. Devillers and R. Poilblanc, *Organometallics*, 1989, **8**, 1308; (*c*) T. Arliguie, B. Chaudret, F. Jalon, A. Otero, J. A. Lopez and F. J. Lahoz, *Organometallics*, 1991, **10**, 1888.

2 (*a*) A. Antinolo, B. Chaudret, G. Commenges, M. Fajardo, F. Jalon, R. H. Morris, A. Otero and C. T. Schweitzer, *J. Chem. Soc., Chem. Commun.*, 1988, 211; (*b*) A. Antinolo, F. Carrillo, J. Fernández-Baeza, A. Otero, M. Fajardo and B. Chaudret, *Inorg. Chem.*, 1992, **31**, 5156; (*c*) A. Antinolo, F. Carrillo, B. Chaudret, J. Fernández-Baeza, M. Lafranchi, H.-H. Limbach, M. Maurer, A. Otero and M. A. Pellinghelli, *Inorg. Chem.*, 1994, **33**, 5163; (*d*) A. Antinolo, F. Carrillo, B. Chaudret, J. Fernández-Baeza, M. Lafranchi, H.-H. Limbach, M. Maurer, A. Otero and M. A. Pellinghelli, *Inorg. Chem.*, 1996, **35**, 7873.

3 D. M. Heinekey, N. G. Payne and G. K. Schulte, *J. Am. Chem. Soc.*, 1988, **110**, 2303; D. M. Heinekey and T. G. P. Harper, *Organometallics*, 1991, **10**, 2891; D. M. Heinekey, N. G. Payne and C. C. Sofield, *Organometallics*, 1990, **9**, 2643; D. M. Heinekey, *J. Am. Chem. Soc.*, 1991, **113**, 6074.

4 D. G. Gusev, R. Kuhlman, G. Sini, O. Eisenstein and K. G. Caulton, *J. Am. Chem. Soc.*, 1994, **116**, 2685.

5 (*a*) B. Chaudret, H. H. Limbach and C. Moise, *C. R. Hebd. Seances Acad. Sci., Ser. 2*, 1992, **315**, 533; (*b*) S. Sabo-Etienne, B. Chaudret, H. Abou el Makarim, J.-C. Barthelat, J.-P. Daudey, S. Ulrich, H.-H. Limbach and C. Moise, *J. Am. Chem. Soc.*, 1995, **117**, 11 602.

6 K. W. Zilm, D. M. Heinekey, J. M. Millar, N. G. Payne and P. Demou, *J. Am. Chem. Soc.*, 1989, **111**, 3088; K. W. Zilm, D. M. Heinekey, J. M. Millar, N. G. Payne, S. P. Neshyba, J. C. Duchamp and J. Szcyrba, *J. Am. Chem. Soc.*, 1990, **112**, 920.

7 D. H. Jones, J. A. Labinger and D. P. Weitekamp, *J. Am. Chem. Soc.*, 1989, **11**, 3087.

8 (*a*) H.-H. Limbach, G. Scherer, M. Maurer and B. Chaudret, *Angew. Chem., Int. Ed. Engl.*, 1992, **31**, 1369; (*b*) H.-H. Limbach, S. Ulrich, G. Buntkowsky, S. Sabo-Etienne, B. Chaudret, G. J. Kubas and J. Eckert, submitted for publication.

9 J. C. Barthelat, B. Chaudret, J. P. Daudey, P. De Loth and R. Poilblanc, *J. Am. Chem. Soc.*, 1991, **113**, 9896.

10 E. Clot, C. Leforestier, O. Eisenstein and M. Pélissier, *J. Am. Chem. Soc.*, 1995, **117**, 1797.

11 A. Jarid, M. Moreno, A. Lledos, J. M. Lluch and J. Bertran, *J. Am. Chem. Soc.*, 1995, **117**, 1069.

12 F. A. Jalon, B. Manzano, A. Otero, E. Villaseñor and B. Chaudret, *J. Am. Chem. Soc.*, 1995, **117**, 10 123.

13 H. H. Limbach, in *NMR Basic Principles and Progress*, Springer, Berlin, 1991, vol. 26, ch. 2; H. H. Limbach, G. Scherer, L. Meschede, F. Aguilar-Parrilla, B. Wehrle, J. Braun, C. Hoelger, H. Benedict, G. Buntkowsky, W. P. Fehlhammer, J. Elguero, J. A. S. Smith and B. Chaudret, in *Ultrafast Reaction Dynamics and Solvent Effects*, eds. Y. Gauduel and P. J. Rossky, American Institute of Physics, AIP Conference Proceedings 298, 1994, Part III, pp. 225–239.

14 V. Bakhmutov, T. Bürgi, P. Burger, U. Ruppli and H. Berke, *Organometallics*, 1994, **13**, 4203.

15 H. Suzuki, D. H. Lee, N. Oshima and Y. Moro-Oka, *Organometallics*, 1987, **6**, 3054.

16 G. J. Kubas, *Inorg. Synth.*, 1982, **19**, 90.

17 R. Uson, A. Laguna and M. Laguna, *Inorg. Synth.*, 1989, **26**, 86.

18 G. S. Denisov and N. S. Golubev, *J. Mol. Struct.*, 1981, **75**, 311; N. S. Golubev, S. F. Bureiko and G. S. Denisov, *Adv. Mol. Relaxation Interact. Processes*, 1982, **24**, 225; N. S. Golubev, G. S. Denisov and E. G. Pushkareva, *J. Mol. Liquids*, 1983, **26**, 169; N. S. Golubev and G. S. Denisov, *J. Mol. Struct.*, 1992, **270**, 263; N. S. Golubev, S. N. Smirnov, V. A. Gindin, G. S. Denisov, H. Benedict and H. H. Limbach, *J. Am. Chem. Soc.*, 1994, **116**, 12 055.

19 G. Binsch, *J. Am. Chem. Soc.*, 1969, **91**, 1304; J. W. Emsley, Feeney and J. L. H. Sutcliffe, *High Resolution Nuclear Magnetic Resonance Spectroscopy*, Pergamon, Oxford, 1965, vol. 1; A. Abragam, *The Principles of Nuclear Magnetism*, Clarendon Press, Oxford, 1961; R. R. Ernst, G. Bodenhausen and A. Wokaun, *Principles of NMR in One and Two Dimensions*, Clarendon Press, Oxford, 1987.

Received 19*th February* 1997; *Paper* 7/01171G